Design and simulation of Hybrid Renewable Energy System for on-grid applications

Ali S. Saleh[1], Rakan Khalil ANTAR[2], Ahmed J. Ali[3]
{ali.alhafidh@ntu.edu.iq[1], rakan.antar@ntu.edu.iq[2], ahmed.j.ali@ntu.edu.iq[3]}

Northern Technical University Technical Engineering College/Mosul, Iraq[1,2,3]

Abstract. A hybrid renewable energy system (HRES) refers to a system that uses a combination of RESs such as wind and PV solar energies to improve and increase energy production and system efficiency. Since one energy source is used to provide electricity, the other one may be available or unavailable. This study is dealt with the design and analysis of a grid connected HRES conversion based on PV solar and wind turbine energy sources that use a DC converter and a permanent magnet synchronous generator. The goal of this work is to suggest a better dc bus voltage regulation approach for PV/Wind power generation systems that are grid-connected. To get a maximum amount of power generation, a maximum power point tracking controller based on Perturb and Observation algorithm is used. This approach improves efficiency and reduces harmonic content problems. The THD value of the output voltage was 0.94%. The HRES is built and modelled by the MATLAB program.

Keywords: hybrid renewable energy system, solar cell, wind turbine, MPPT, Boost Converter, H-bridge inverter.

1 Introduction

The most pressing challenge in recent decades has been the efficient utilization of renewable energy sources. As a result of increased energy demand and limited fossil fuel resources, pollutants and save on fuel expenses have been reduced. Renewable Energy Systems (RESs) are getting popular and becoming more economically effective than traditional energy generation systems for supplying dependable energy in areas where conventional power grids are not available [1],[2]. RESs are inherently changeable and fluctuate, and often provide little power as compared to traditional power generation. As a result, to supply more dependable and sustainable energy, a way of combining varied sources is required [3]. A hybrid RES (HRES) is formed by the combination of multiple RESs, which provides continuous electricity to customers as opposed to a system that is based on a single source [4],[5]. Power converters are used in HRES to allow flexible and effective connectivity of RESs and to utilize in either grid-connected or standalone mode. Nonetheless, the HRES cannot deliver adequate and consistent electricity to fulfil the demand power due to the random and unpredictable nature of PV and wind systems [6]. To assure the HRES's dynamics, certain reliable power sources such a fuel cells (FC) [7], batteries, diesel generators, or super capacitors[8], must be included in the HRES particularly in "standalone" mode and in the utility in "grid-connected" mode. Various hybrid

IMDC-IST 2021, September 07-09, Sakarya, Turkey

DOI 10.4108/eai.7-9-2021.2314947

grid-connected circuit topologies illustrated in Figure (1) depict the Wind/PV energy system [9]. Figure 1(a) illustrates a grid-connected hybrid Wind/PV generation system with two separate converters dc/dc/ac that is ac-shunted. Each of them can deliver the maximum amount of energy generated by the PV solar or wind turbine (WT). However, because solar and wind power are complementary, the circuit architecture depicts in Fig 1(a) may be simplified to another type as illustrated in Fig.1(b). The two dc-dc converters are relocated and linked in parallel. The overall power ratings of the two separate dc-ac inverters are larger than the output power of the dc-ac inverter for the dc-shunted grid-connected power system[10]. It has the potential to shrink the size and expense of the power system. However, the circuit architecture illustrated in Fig. 1(b) may be reduced even further, as illustrated in Fig. 1(c) where the two separate converters are replaced with a multi-input (MI) dc-dc converter.

The following survey gives an idea about some studies that deal with wind and solar units. In 2015 [11], a hybrid distributed generator topology based on solar and wind-powered PMSG was presented. Only one single boost converter and inverter are used to connect the sources to the grid. A model of the suggested strategy is created in the d-q axes reference frame. For the new hybrid scheme, two low-cost controllers are proposed to individually activate the converter DC-DC and the inverter. The generator's voltage and current THD meet IEEE's recommended power quality standards. In 2016[12], a hybrid power monitoring and management laboratory-scale system for micro-grids dependent on wind, solar, and batteries was suggested. The system is intended to regulate the operation of PV solar panels using MPPT. The wind energy conversion system (WECS) is managed by a feedback control rule for speed following. In 2017 [13], a hybrid renewable energy system was presented. Power converters are used to connect the wind turbine, solar panel, supercapacitor, and battery storage to a DC connection. To accomplish operating PowerPoint taking instead of MPPT, wind and solar sources are coupled to corresponding converters with a boost. In 2019 [14], two micro-grid-linked PMSG wind turbine systems were examined. In the first concept, a rectifier circuit with a filter-boost converter and a common DC bus is linked to the PV solar, WT, and batteries banks. In the second path, an inverter circuit is used to connect both the PV array and the storage batteries. The WT is connected to the three-phase AC directly via a back-to-back conversion and a step-down transformer. The first model, according to simulation findings, provides higher power quality and reduced voltage harmonics. The second model can provide more residential supply due to the performance of the advanced transformer and inverter. In 2020 [15], a solar-wind hybrid system was designed and analysed. The alternating energy of the wind generator is transformed to a constant DC value that may be utilized to charge the batteries or subsequently converted to AC voltage to operate AC loads using an AC-DC inverter. A boost converter based on the MPPT system is designed to extract the most power feasible. This method gives greater harmonic reduction. As mentioned in the previous study, a HERS shown in Fig. 2 is suggested and adopted in this study.

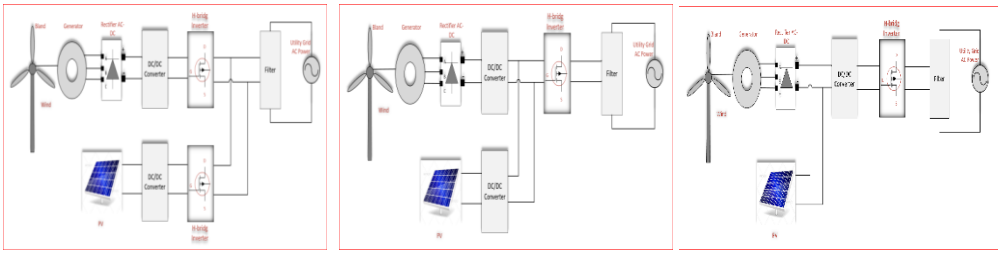

(a) (b) (c)

Fig 1. Circuit Topologies available For ON-Grid Utility Hybrid PV/Wind Power Plant generation system with (a) ac-shunting and (b) with dc-shunting. (c) MI grid-connected system.

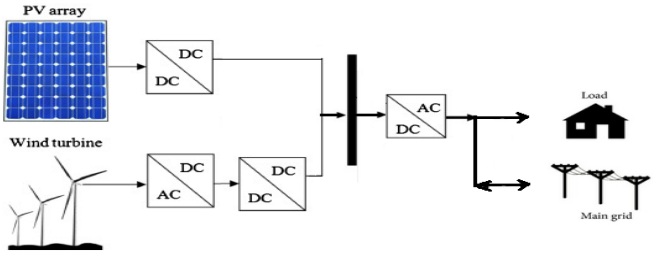

Fig 2. Suggested circuit of the wind- PV Hybrid System.

2 Design of Hybrid Wind/PV Power generation System

The planned HRES is divided into solar energy conversion, wind energy conversion system with PMSG, DC-DC converter based on MPPT algorithm, and full-bridge inverter with SPWM control. The suggested system's block diagram is represented in Fig. (3). The HRE with solar and wind systems is designed with two synchronous boost converters running in parallel. The two units are modelled and simulated by MATLAB software to generate an output voltage with low distortion. The implemented model has a low cost and a simpler design. The controller is configured to balance the H-bridge inverter input voltage by controlling the inputs of both the PV solar panel and the wind turbine through the boost converter by using the P&O MPPT algorithm. The following is a description of the complete system modelling.

2.1 Modelling of PV Cell

PV cells are basically like a large area p-n junction of the diode. The equivalent circuit of the PV cell is depicted in Fig(4). The PV cell mathematical model may be established using MATLAB/Simulink. The characteristics of the Solar PV (P-V and I-V curve) depicted in Fig.(5) is characterized according to the PV current equation below [16],[17].

$$I = I_{pv} - I_o\left[exp\left(\frac{q(V+I)}{N_{ser}\times K\times T\times a}\right) - 1\right] - \frac{V+I\times R_s}{R_{sh}} \quad (1)$$

where I_{pv} , V_t , I_o , a, R_{sh} , R_s, k, T, and q are PV current, array thermal voltage, saturation current, the ideality element of diode's, series and parallel resistance of the array, Boltzmann's constant, temperature, and the charge of electron respectively. The PV rating voltage can be increased through connects extra cells in series (U_{ser}), whereas the current rating can be improved by producing more parallel connections (N_p). Since R_s is low and R_{sh} is high, the panel's short circuit current is exactly equivalent to the PV panel current. Irradiation and temperature factors affect the current provided by PV, which is expressed as [18]:

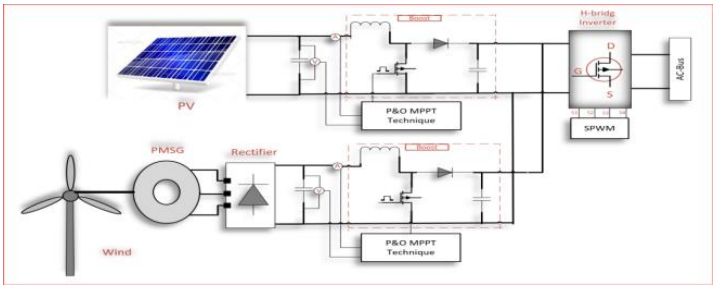

Fig 3. Suggested the system's block diagram for HRE.

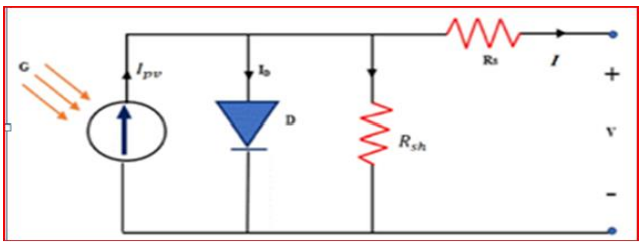

Fig 4. A photovoltaic cell's equivalent circuit

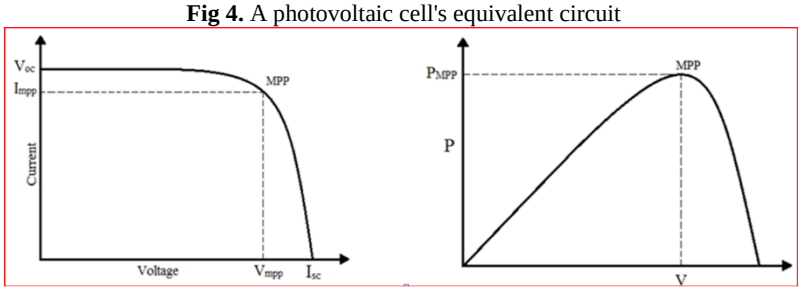

(a) (b)

Fig 5. (a) I-V, (b) P-V features of the PV cell

$$I_{pv} = \left(I_{pv,st} + K \times \Delta T\right)\frac{G}{G_{st}} \tag{2}$$

where $I_{pv,st}$, ΔT , G_{st} and G denote the induced current at normal temperature and irradiance of PV, temperature variation concerning typical one, standard irradiation, and irradiance.

$$I_o = I_{o,st}\left(\frac{T_{st}}{T}\right)^3 exp\left[\frac{q \times E_g}{a \times K}\left(\frac{1}{T_{st}} - \frac{1}{T}\right)\right] \tag{3}$$

where E_g, $I_{o,st}$, T and T_{st}, represent semiconductor bandgap energy, standard temperature, saturation current under standard conditions, and actual temperature, respectively [19]. Furthermore, $I_{o,n}$ can be written as:

$$I_{o,n} = \frac{I_{sc,n}}{exp\left(\frac{V_{oc,n}}{a \times V_{t,n}}\right) - 1} \tag{4}$$

2.2 Modelling of PMSG

The PMSG is created by projecting its equations onto a reference coordinate system that rotates in time with the magnet flux. A phase-locked loop (PLL) is utilized to synchronize the d-q rotating reference frame with the ABC three-phase frame [20]. After that, the following is a dynamic model of the surface-mounted PMSG [21].

$$V_{ds} = R_s.i_{ds} + L_s\frac{di_{ds}}{dt} - \omega.\Psi_{qs} \quad (5)$$

$$V_{qs} = R_s.i_{qs} + L_s\frac{di_{qs}}{dt} + \omega.\Psi_{ds} \quad (6)$$

Where L_s, R_s, w, Ψ_{ds}s and Ψ_{qs} are the generator inductance and resistance, electrical generator speed, and the d-q axis magnet flux, which are represented as follows:

$$\Psi_{ds} = L_s.i_{ds} + \varphi \quad (7)$$

$$\Psi_{qs} = L_s.i_{qs} \quad (8)$$

Where φ is the flux of the magnet. In the synchronous reference frame, the electrical model of PMSG may be represented as follows:

$$\frac{di_{ds}}{dt} = \frac{1}{L_s}\left(-R_s.i_{ds} + \omega \times L_s.i_{qs} + V_{ds}\right) \quad (9)$$

$$\frac{di_{qs}}{dt} = \frac{1}{L_s}\left(-R_s.i_{qs} - \omega.L_s.i_{ds} - \omega.\varphi + V_{qs}\right) \quad (10)$$

The electromagnetic torque of PMSG's non-salient poles is expressed as:

$$T_{em} = \frac{3}{2}.p.\varphi.i_{qs} \quad (11)$$

Where p is the number of pole pairs in the generator. Eq.(10) demonstrates that the q_{axis} current in the stator may be used to adjust the generator torque directly. The following statement may be used to define the mechanical dynamics model of the specified wind turbine system:

$$j_T.\frac{d\omega_r}{dt} + \mathrm{f}.\varphi_r = T_T - T_{em} \quad (12)$$

where T_T, j_T, f, and ω_r denoted as mechanical torque, a moment of inertia, coefficient of friction, and mechanical speed, which is connected to electrical rotating ω as follows:

$$\omega = \mathrm{p}.\omega_r \quad (13)$$

The WT dynamic model with PMSG is built using MATLAB/Simulink. The system has been implemented to make sure the model and the proposed control techniques. The input of the WT is wind, and the output is mechanical power that moves the generator rotor. The following formulae for a variable speed wind turbine provide the output mechanical power and torque generated by a wind WT turbine [22].

$$P_{mec} = \frac{1}{2}.\rho.\pi.R^2.C_p(\lambda,\beta).v_w^3 \quad (14)$$

$$T_{mec} = \frac{P_{mec}}{w_{mec}} \quad (15)$$

The power coefficient (C_p) for the WT is also a function of the tip speed ratio (λ), blade pitch angle (β) (in degree) which is defined by [23]:

$$C_p(\lambda,\beta) = 0.5\left(\frac{116}{\lambda_i} - 0.4 * \beta - 5\right) e^{-\frac{21}{\lambda_i}} \quad (16)$$

Where λ is defined to be the ratio between the turbine speed (w) and the wind speed (v_w) and is given by.

$$\lambda = \frac{R*\omega_m}{v_w} \quad (17)$$

Consequently, equation (17) can be used to calculate the mechanical angular speed of a turbine, which represents the relationship between mechanical and electrical torque, incorporating the generator and turbine masses:

$$J * {dw_{mec}}/{dt} = T_{elc} - T_{mec} - B_{mec}.* w_{mec} \quad (18)$$

Fig 6 shows the whole Simulink wind turbine model for wind turbines may be created using the equations descript from (13) to (15). This figure shows that for a certain wind velocity (v_w), the generated power by turbines (P_{mec}) is affected by the value of C_p, air density (ρ), and parameters of the turbine. The density of the air and the characteristics of the turbine (which are defined by the design) are constant [24]. As a result, in a turbine with a fixed blade pitch angle, the output power has been mostly depending on the value of C_p, which is determined by the wind turbine's rotor speed. As a result, when C_p is in the great value, the output power of the wind turbine is maximum. This ideal value of C_p occurs with various values of λ as shown in equation (16). For a given wind speed, there will be only one ideal rotor speed where the C_p is at maximum value. The factor C_{p_max} is obtained at optimal value of (λ_{opt}) to maximize the extracted power. Fig 7 shows C_p at its maximum value (C_{p_max}) and λ at its optimum value (λ_{opt}).

The amplitude and frequency of the voltage output from a PMSG vary for a variable speed wind turbine when the wind speed changes from time to time, while in this circumstance the generator power output should be stabilized. Therefore, PMSG with wind turbine in this configuration is linked to the DC bus through a three-phase rectifier, as illustrated in Fig 2. The WECS is connected to a rectifier followed by a filtered-DC boost converter circuit based on the MPPT algorithm and P&O method. The parameters of the wind turbine system with a PMSG, used in the simulation, are presented in Table 1. A PMSG WT is modelled in a Simulink environment as seen in Fig 8. The mechanical torque T_m is generated by feeding the wind and rotor speeds into the control block.

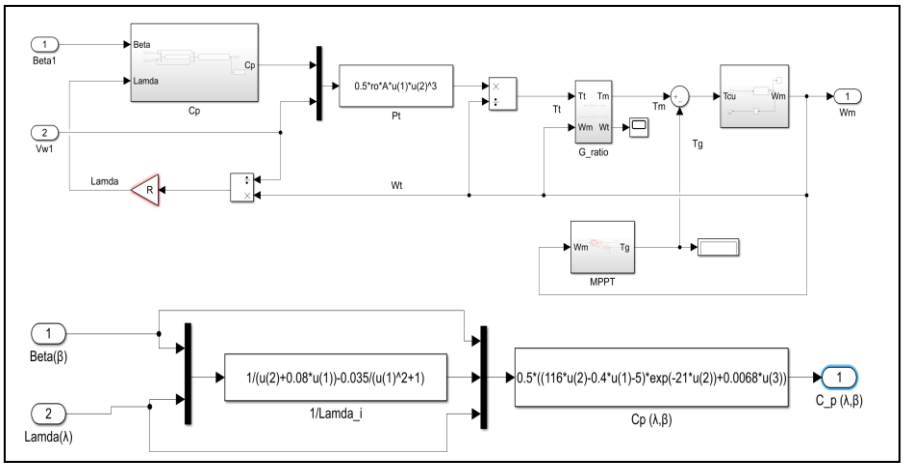

Fig 6. MATLAB Block Diagram of a Wind Turbine.

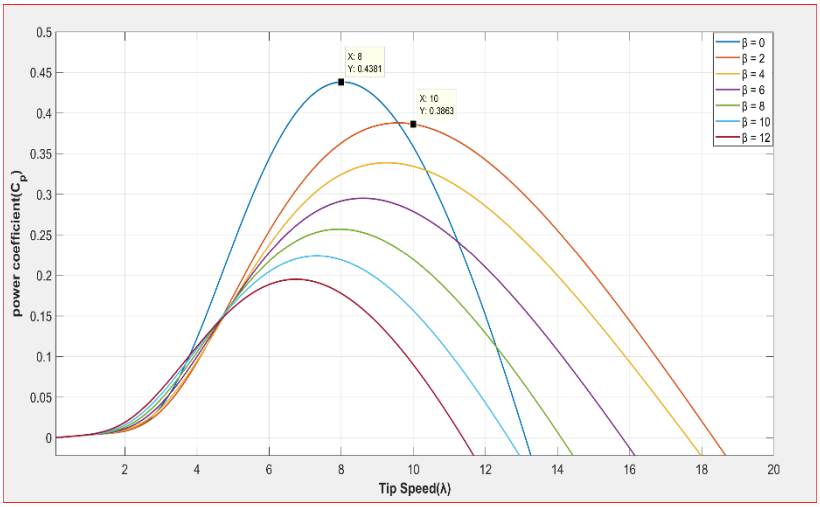

Fig 7. The maximum value of (C_p) and the optimum value of (λ).

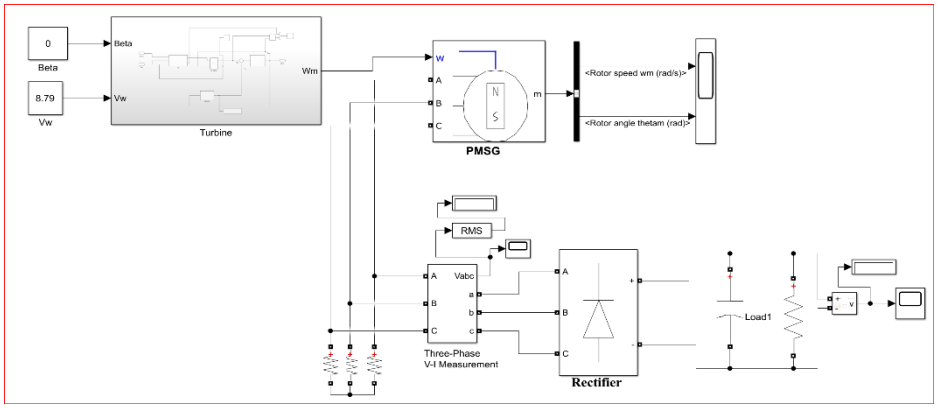

Fig 8. Modeling of the Turbine System using MATLAB.

Table 1. Simulation Parameters of the PMSM

Value	Parameters
1000 (w)	Rated power
1500 (rpm)	Rated speed
240 (V)	Output voltage
3	Number of phases
10	Number of poles
15	Number of coils
1.2 Ω	stator phase resistance,
0.000835H	Inductance
7[mm]	Thickness of PM
1000 (w)	Rated power

2.3 DC-DC Boost Converters

The boost converter circuit is often used as an interface device between load and PV panel, where the PV output is combined with the load to obtain maximum power. It converts the magnitude of the input DC voltages to variable DC voltages. The power circuit of the boost converter used in this study is shown in Fig (9). The duty ratio is used to regulate the output voltage provided by the boost converter circuit.

$$V_o = \frac{V_{in}}{1-D} \tag{19}$$

where D, V_{in} and V_o are duty ratio, input, and output DC voltage. The following calculations are used to quantify and choose the inductor and capacitor values of a boost converter [25].

$$L = \frac{V_{in}}{f_{sw} \times (\Delta I_l) D} \tag{20}$$

$$C = \frac{I_o}{f_{sw} \times (\Delta V_o) D} \tag{21}$$

Where ΔI_l , f_{sw} and ΔV_o are the ripple of input current, switching frequency, and output voltage ripple respectively. To increase utilization of the PV panel, A MPPT method is employed. As the power provided by these panels varies constantly with environmental conditions like temperature and irradiance, this technique is critical for ensuring the transition of the maximum power from PV to load. Many different techniques such as constant voltage, open voltage, P&O, neural network, fuzzy logic control, and incremental conductance have been developed to optimize the generation of solar energy [26]. These strategies vary in terms of difficulty, expense, level of effectiveness and tracking speed, popularity, hardware, and so on. An accurate cost analysis of this MPPT algorithm can be prepared by understanding the method (analogy or digital) used in the control system, the number of used sensors, and any additional power components, while keeping all additional costs (power components, electronic components, boards...) constant overall systems[27]. In this paper, the P&O technique is used because of its

simplicity and required only one sensor. The algorithm is formed by perturbing a small increment in voltage of PV and observing the power change. Figure (10) illustrates a flowchart of the P&O method [28].

2.4 Power Inverter

The inverter is an electrical circuit that enables a voltage to be applied in both directions along with a load. The H-Bridge is created by combining four solid-state switches and controlled based on the pulse width modulation (SPWM) method. A sinusoidal with a triangle waveform is compared to creating this sort of signal.

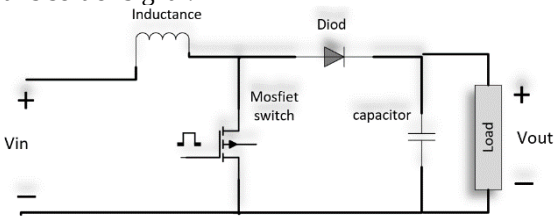

Fig. 9. Boost converter circuit.

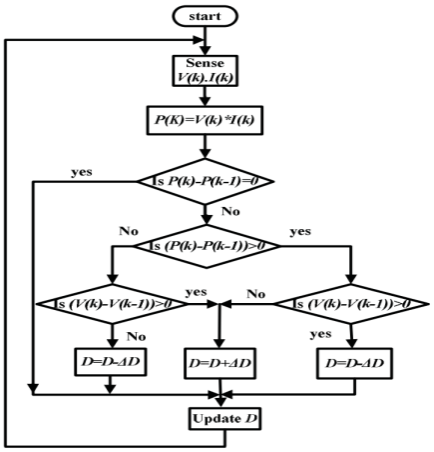

Fig 10. Flowchart of the PO algorithm[28].

3 Modelling and Simulation of Grid-Connected HREs

A circuit diagram of a dc/dc boost converter, filters for the dc bus, inverter (full bridge), and an abased controller is shown in Fig (11). The input dc-dc boost converter may transmit the electricity generated by the PV array and WT to the dc bus separately or simultaneously. If one of the energy sources fails, the other dc/dc boost converter can still transmit the required power to the dc bus from the other energy source. The MPPT functionality is available for both the PV array and the WT. The inverter creates a sinusoidal AC and injects it into the grid or load or both. A grid-connected hybrid may simultaneously supply energy to both the load and the utility grid at the same time. When it is linked to the grid, suitable power electronic controllers are necessary to manage voltage, frequency, and harmonic regulations, as well as load sharing. In

the proposed model, a grid is added with the model so that unused power can be supplied to the grid. The MPPT controllers are suggested for operating wind and PV generators at maximum power, which improves the amount of energy captured from wind speed and solar radiation. To optimize the output power of the PV and wind generator, an MPPT controller is P&O included in the system. The PWM inverter is used to maintain the inverter's output voltage at the rated voltage regardless of the output load. A voltage control strategy is proposed for this single-phase inverter to regulate the DC bus voltage to a constant value of 311V. The control loop is depicted in Fig (12). To fix the magnitude inverter voltage and synchronized with the grid, a comparison between the inverter output voltage and the grid voltage is made where the angle between the inverter's AC output voltage (Vinv) and the grid's AC voltage (Vgrid) is regulated by a single-phase lock loop to adjust inverter frequency with grid frequency. To modify the required output voltage, the reference grid side voltage can be established in the controller.

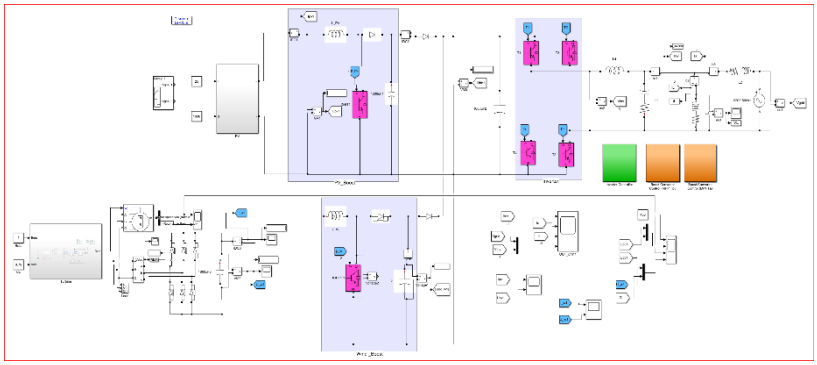

Fig 11. The architecture of a typical wireless sensor node.

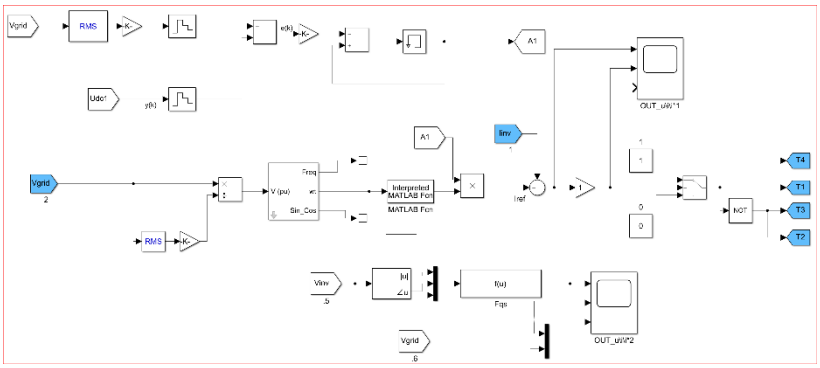

Fig 12. Control of Gating Signals for on-Grid Inverters.

4 Results of the Simulation

The HRES is simulated using MATLAB/Simulink software, where the work is divided into several stages, according to the load source fitted at standard test weather conditions, changing weather conditions, and the disturbance in the load (increase or decrease). In the first stage, the system is tested under standard weather conditions (1000W/m^2 insolation and 25℃ temperature), wind speed of 8 m/sec, and load value of 150 ohms. Figure 13 depicts the boost

converter's output voltage as well as the input voltage responses (PV and wind HREs). The graph demonstrates that the output voltage is relatively steady and equal to 311V. Fig 14 depicts the waveform of a centralized inverter of HREs supplies electric power to both the load and the utility grid. therefore, the phase difference between the inverter current and the grid current is 180 degrees. The output waveform of the inverter (V_{inv}) is synchronized with the grid voltage. The total inverter current is 10A, where the load is consumed 2A, and 8A is sent to the grid when the load is 150 ohms. Under the same conditions, the system is tested when a disturbance occurs on the load (decreasing resistance to 70 ohms). Fig 15 shows the waveform of the load current that consume 4.4A and the grid that draws 5.6A

Finally, it is assumed a natural fluctuation occurs on the renewable energy sources which cause a reduction in the generated power of wind/ PV sources. The decrease in renewable power is achieved due to fluctuations in weather conditions (irradiation, temperature, and wind speed). HREs and grid currents are used to supply the load in this scenario. The system is simulated under the weather conditions (400W/m^2 insolation and 25C temperature) and wind speed (3m/sec – 21.5 rad/sec). This leads to the load current is greater than the inviter current. The boost converter output and the input voltage responses (PV and wind HREs) at 70ohm are illustrated in Fig 16. This figure illustrates that the output voltage is constant and equal to 311v, while the inverter current of HREs and grid current are sharing between them to supply the load with the required power. The waveform of the output voltage for the inverter (V_{inv}) is synchronized with the grid voltage as shown in Fig 17a. The total load current, inverter current, and grid current at a load of 70 ohms are 4.4A, 2.8A, and 1.6A, respectively. Figure (17b) shows the FFT analyser for voltage and current of the output inverter.

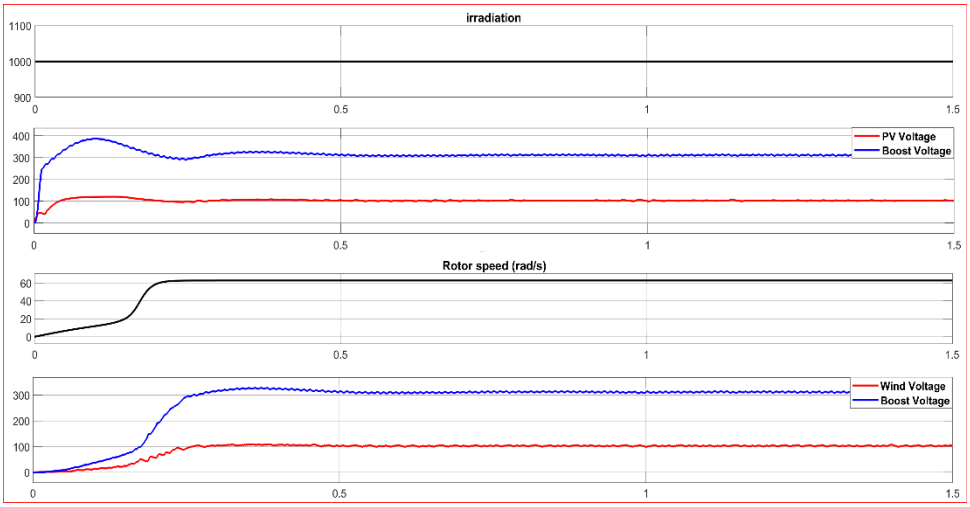

Fig 13. Input and Output Voltage Response of the Boost Converter Based on PV and Wind HRES.

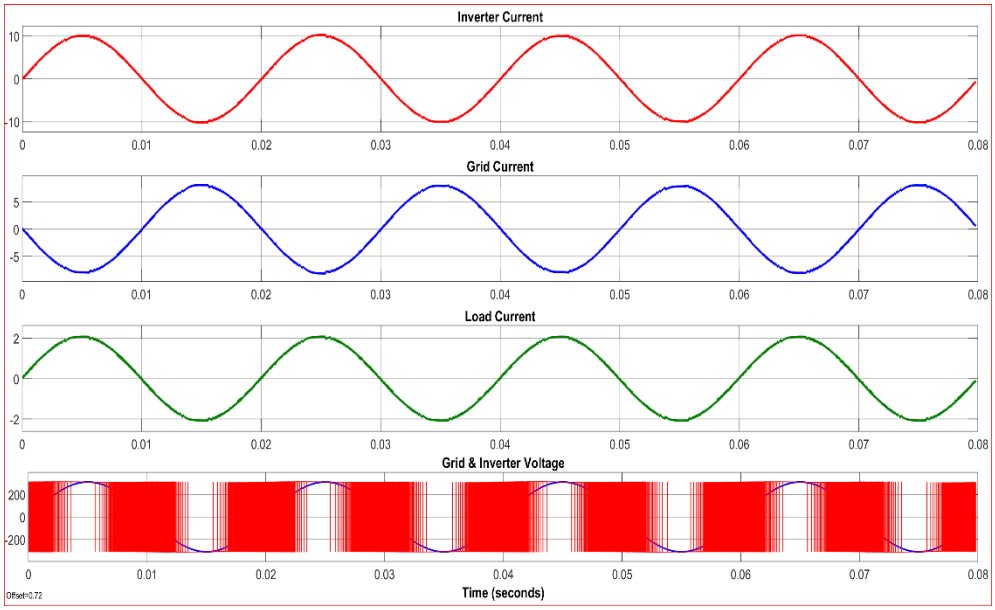

Fig 14. HREs Currents that Supplies Load and Grid with Voltage Centralized with an inverter at 150ohm.

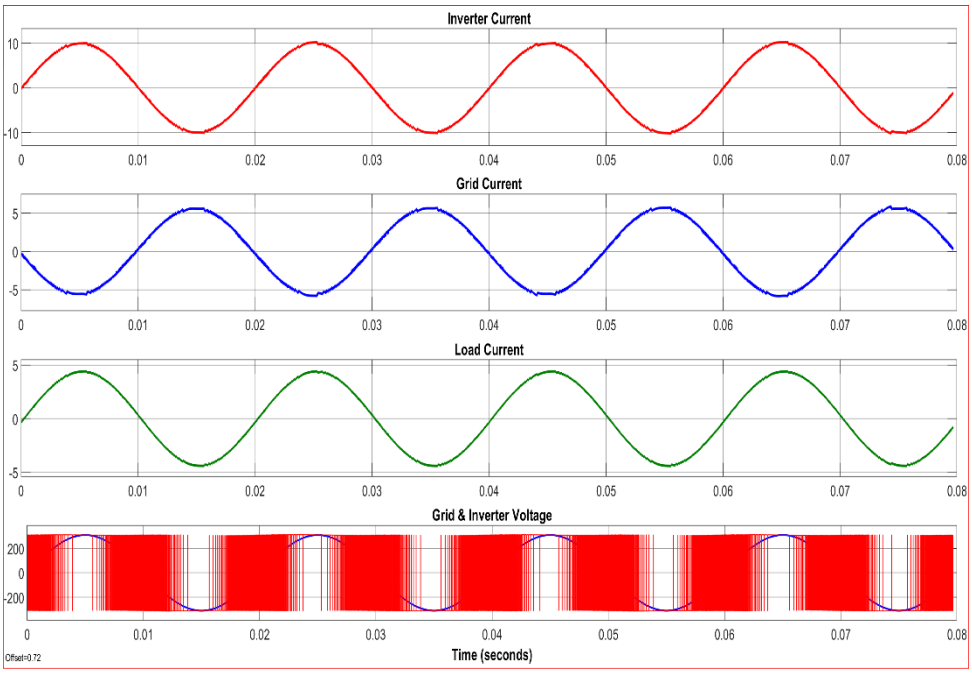

Fig 15. HREs Currents that Supplies Load and Grid with Voltage Centralized with an inverter at 70 ohms.

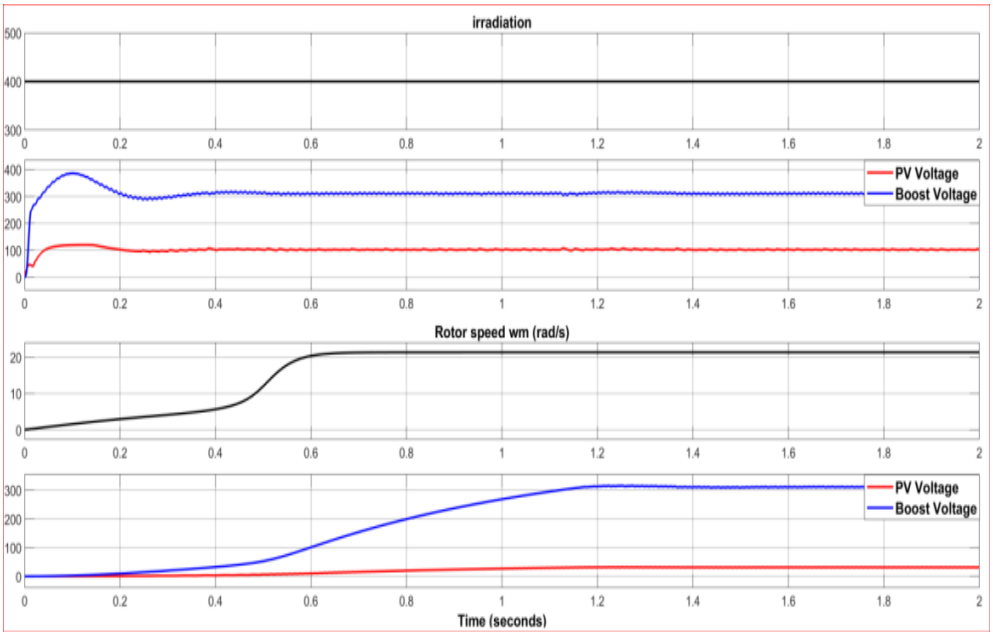

Fig 16. Input and Output Voltage of the Boost Converter.

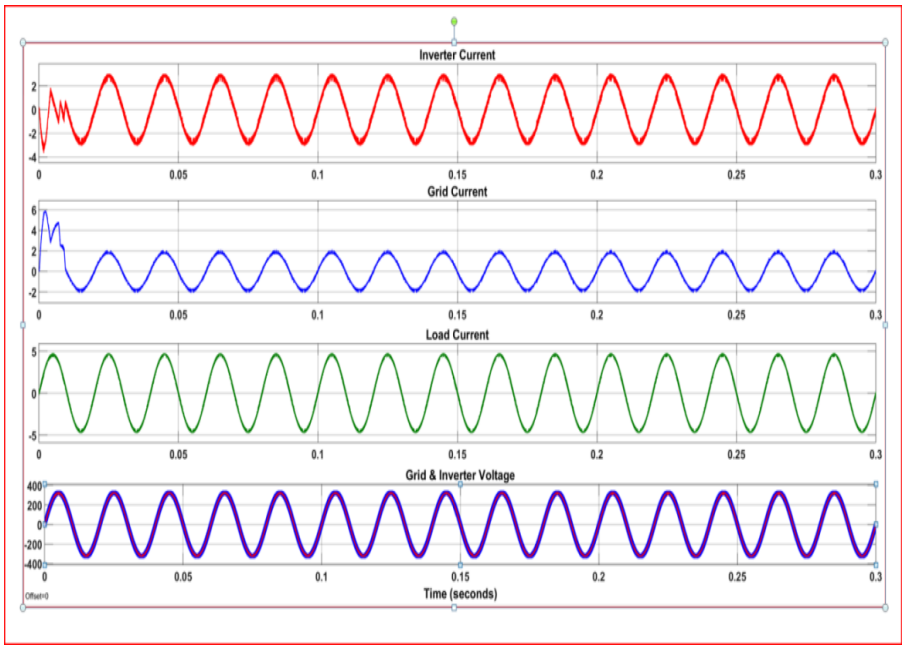

(a)

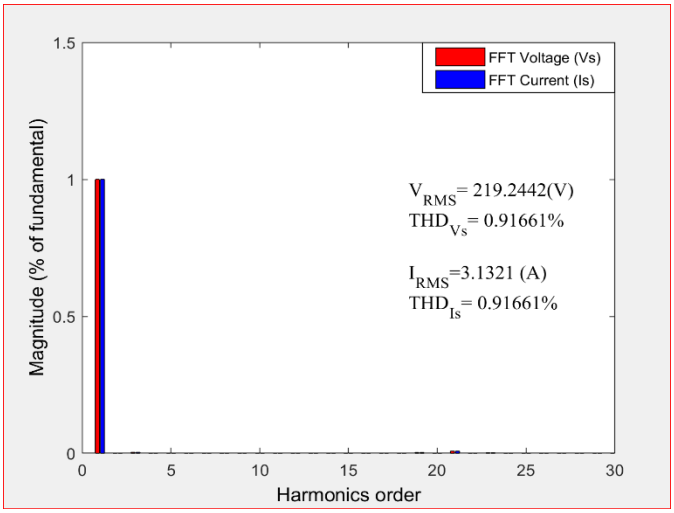

(b)

Fig 17. (a) HREs and grid currents sharing to supply load, (b) FFT analyser of inverter output voltage and current.

5 Conclusion

In current work, an HRES which is consists of two types of RESs (PV module and a wind turbine connected by PMSG) has been designing and simulated to compensate for the deficit that occurs, as well as to reduce the cost of preparing the electric power generated by the traditional electric power system. Also. It is used to improve the quality and quantity of the generated power. The generated power of the PV module is connected to the load via a common DC bus that links through a DC-DC boost converter. While the WT PMSG is connected directly to the DC bus side through a separate DC-DC boost converter after converting the AC output of the PMSG to DC by using a three-phase rectifier. In addition, two separate MPPT algorithms are used to maximize the generated power from the two RES. The output power of the two boost converters is connected to the common DC bus to supply a single phase SPWM inverter that is used to feed a generated power to the load. The hybrid system is modelled using MATLAB/Simulink. To check the ability of the suggested HRES to supply the shortage in the required power, different operating conditions are considered. Three PV modules are selected and connected in series to get an input voltage of 110V. To adjust the output voltages of both PV and wind turbine generators, the MPPT algorithm based on the P&O technique has been used. In addition, an SPWM technique has been used to produce the gate signals of the single-phase inverter. The system is tested with varying input parameters of solar radiation, wind speed, and temperature. The obtained results show that the simulated model has acceptable performance, and it is having the ability to fill the shortage in the supply of electricity. Moreover, the THD values of the simulated systems are lay within standards limits.

References

[1] Ali, A. J., Suliman, M. Y., Khalaf, L. A., Sultan, N. S., "Performance investigation of stand-alone induction generator based on STATCOM for wind power application", International Journal of

Electrical & Computer Engineering, (2088-8708), 10(6), 2020.
[2] A. Ghafoor and A. Munir, “Design and economics analysis of an off-grid PV system for household electrification,” Renew. Sustain. Energy Rev., vol. 42, pp. 496–502, 2015.
[3] B. L. Yong, D. B. Chia, R. K. Rajkumar, V. K. Ramachandaramurthy, and J. Pasupuleti, “Operation and management of an islanded mode hybrid power system e a Malaysian perspective,” 2010.
[4] R. K. Rajkumar, V. K. Ramachandaramurthy, B. L. Yong, and D. B. Chia, “Techno-economical optimization of hybrid pv/wind/battery system using Neuro-Fuzzy,” Energy, vol. 36, no. 8, pp. 5148–5153, 2011.
[5] P. Thounthong, S. Sikkabut, P. Sethakul, and B. Davat, “Control algorithm of renewable energy power plant supplied by fuel cell/solar cell/supercapacitor power source,” in The 2010 International Power Electronics Conference-ECCE ASIA-, 2010, pp. 1155–1162.
[6] A. N. Hussain, A. J. Ali, F. S. Ahmed,"Power quality improvement based on hybrid coordinated design of renewable energy sources for DC link channel DSTATCOM", International Journal of Electrical & Computer Engineering, (2088-8708) 10.5 (2020).
[7] Rakan Khalil Antar, Nashwan S. Sultan, Ahmed J. Ali, "Speed Control of Three-Phase Induction Motor Fed by Renewable Energy Source", 2nd International Conference on Electrical, Communication, Computer, Power and Control Engineering (ICECCPCE), Mosul, Iraq, IEEE 2019, pp.7–12, doi:10.1109/ICECCPCE46549.2019.203739.
[8] G. Tian, X. Ding, and J. Liu, “Study of control strategy for hybrid energy storage in wind-photovoltaic hybrid streetlight system,” in 2011 IEEE international workshop on open-source software for scientific computation, 2011, pp. 77–81.
[9] Y.-M. Chen, C.-S. Cheng, and H.-C. Wu, “Grid-connected hybrid PV/wind power generation system with improved DC bus voltage regulation strategy,” in Twenty-First Annual IEEE Applied Power Electronics Conference and Exposition, 2006. APEC’06., 2006, pp. 7-pp.
[10] Rakan Khalil Antar, Basil M. Saied, Rafid A. Khalil, “Using seven-level cascade H-bridge inverter with HVDC system to improve power quality”, First National Conference for Engineering Sciences (FNCES), Baghdad, Iraq, IEEE, pp. 1-7, 2012, doi:10.1109/NCES.2012.6740457.
[11] M. M. R. Singaravel and S. A. Daniel, “IEEE TRANSACTIONS ON INDUSTRIAL ELECTRONICS MPPT with Single DC-DC Converter and Inverter for Grid Connected Hybrid Wind-Driven PMSG-PV System,” vol. 0046, no. c, 2015, doi: 10.1109/TIE.2015.2399277.
[12] A. Merabet, K. T. Ahmed, H. Ibrahim, R. Beguenane, and A. M. Y. M. Ghias, “Energy management and control system for laboratory scale microgrid based wind-PV-battery,” IEEE Trans. Sustain. energy, vol. 8, no. 1, pp. 145–154, 2016.
[13] R. Sharma and S. Suhag, “Novel control strategy for hybrid renewable energy-based standalone system,” Turkish J. Electr. Eng. Comput. Sci., vol. 25, no. 3, pp. 2261–2277.
[14] K. Tazi, M. F. Abbou, and F. Abdi, “Performance analysis of micro-grid designs with local PMSG wind turbines,” Energy Syst., pp. 1–33, 2019.
[15] G. M. S. U. Al-Mamun, M. R. Hasan, M. I. Hossain, A. A. Atik, S. M. D’ Al Jubair Hossain, and A. R. A. S. M. Costa, “Design and Analysis of a Solar-Wind Hybrid System.”
[16] A. S. Saleh, R. K. Antar, and A. J. Ali, “Design and Implementation of Single-Phase PV Power System,” Ann. Rom. Soc. Cell Biol., vol. 25, no. 6, pp. 12078–12087, 2021.
[17] H. M. Ridha, C. Gomes, H. Hizam, M. Ahmadipour, D. H. Muhsen, and S. Ethaib, “Optimum design of a standalone solar photovoltaic system based on novel integration of iterative-PESA-II and AHP-VIKOR Methods,” Processes, vol. 8, no. 3, 2020, doi: 10.3390/PR8030367.
[18] A. M. T. IbraheemAlnaib, “Simulation and Characteristics Study of Solar Photovoltaic Array using Matlab/Simulink,” J. Tech., vol. 29, no. 1, 2016.
[19] M. T. Chughtai, “Temperature compensated bias supply circuit for photodiodes,” Przegląd Elektrotechniczny, vol. 94, no. 10, pp. 207–209, 2018.
[20] S.-K. Chung, “Phase-locked loop for grid-connected three-phase power conversion systems,” IEE Proceedings-Electric Power Appl., vol. 147, no. 3, pp. 213–219, 2000.
[21] F. Khater and A. Omar, “A review of direct driven PMSG for wind energy systems,” J. Energy

Power Eng., vol. 7, no. 8, 2013.
[22] H. I. Karim Belmokhtar and M. L. Doumbi, “A Maximum Power Point Tracking Control Algorithms for a PMSG-based WECS for Isolated Applications: Critical Review,” Wind Turbines Des. Control Appl., p. 199, 2016.
[23] S. H. Chichester and J. Hindmarsh, “Grid integration of wind energy conversion systems,” Wiley, 385p, 1999.
[24] Z. M. Abdullah, A. M. T. I. Alnaib, and O. T. Mahmood, “Design of Wind Turbine Energy System Based on Matlab/Simulink,” Eng. Tech. J., vol. 32, 2014.
[25] E. Mattos, A. M. S. S. Andrade, G. V. Hollweg, J. R. Pinheiro, and M. L. da Silva Martins, “A review of boost converter analysis and design in aerospace applications,” IEEE Lat. Am. Trans., vol. 16, no. 2, pp. 305–313, 2018.
[26] T. C. C. Saibabu and J. S. Kumari, “Modeling and simulation of pv array and its performance enhancement using MPPT (P&O) technique,” IJCSCN, vol. 1, pp. 9–16, 2011.
[27] J. Chauhan, P. Chauhan, T. Maniar, and A. Joshi, “Converters Based Photovoltaic Systems,” pp. 476–481, 2013.
[28] B. Sah and G. V. E. S. Kumar, “A comparative study of different MPPT techniques using different dc-dc converters in a standalone PV system,” in 2016 IEEE Region 10 Conference (TENCON), 2016, pp. 1690–1695.